journal

J. Am. Ceram. Soc., 94 [1] 250–254 (2011)
DOI: 10.1111/j.1551-2916.2010.04037.x

Fabrication and Characterization of High-*k* Dielectric Nickel Titanate Thin Films Using a Modified Sol–Gel Method

Shiow-Huey Chuang,[†,‡] Min-Lung Hsieh,[‡] Shih-Chieh Wu,[§] Hong-Cai Lin,[‡] Tien-Sheng Chao,[¶] and Tuo-Hung Hou[§]

[‡]Department of Applied Chemistry, National University of Kaohsiung, Kaohsiung, Taiwan 81148, ROC

[§]Department of Electronics Engineering & Institute of Electronics, National Chiao-Tung University, Hsinchu, Taiwan 30010, ROC

[¶]Department of Electrophysics, National Chiao-Tung University, Hsinchu, Taiwan 30010, ROC

This research produced high-quality, single-phase nickel titanate ($NiTiO_3$) thin films, a high-*k* material for gate dielectrics, by a modified sol–gel method. The precursor was prepared by reactions of nickel acetate tetrahydrate and titanium isopropoxide in 2-methoxyethanol with a 1:1 ratio of Ni/Ti in the solution. After coating, the films were post-heat treated between 500° and 900°C. X-ray diffraction indicated that the films deposited at and above 600°C were single-phase nickel titanate. X-ray photoelectron spectra of a typical thin film revealed that the binding energies of Ni $2p_{3/2}$ and Ti $2p_{3/2}$ electrons were 855.2 and 457.7 eV, respectively. Raman spectra showed eight absorptions between 200 and 800 cm^{-1}. Scanning electron microscope images showed smooth surfaces. Findings showed the dielectric constant of the $NiTiO_3$ film to be 41.36 by capacitance–voltage analysis. The results show that single-phase $NiTiO_3$ film can be prepared by the sol–gel spin coating method and then heat-treated at 600°C.

I. Introduction

METAL titanate-based Perovskite-type oxides, including metals such as nickel, cobalt, barium, strontium, ferrite, lead, zinc, and copper, have received considerable research interest in recent years due to their chemical and electrical properties. These materials are widely used in gas-sensors,[1,2] humidity sensors,[3–5] magnetic recording media,[6] catalysts,[7–10] and other applications. Metal titanates have recently drawn attention as a promising high dielectric material, which can be used in semiconductor devices like dynamic random access memories, and metal-oxide semiconductor field-effect transistors to solve current leaking problems.[11–14] Metal titanates can also be used in organic thin-film transistors to solve charge transport problems between different layers,[15] and applied in ferroelectric random access memory due to their excellent ferroelectric properties.[16–19]

Nickel titanate materials have been prepared previously by solid-state reactions with a process temperature of over 1000°C.[20] Several studies have explored various methods to reduce the reaction temperature when preparing nickel titanate. Unfortunately, the $NiTiO_3$ preparation process results in the formation of an unwanted byproduct, titanium oxide (TiO_2). Several different methods, such as nanoparticle-directed solid-state synthesis,[21] a wet-chemistry synthesis method,[22] a polymeric precursor method,[23] and a modified Pechini process,[20] have aimed at mitigating this problem and producing pure $NiTiO_3$. However, even when the temperature was as low as 600°C, these methods were only available to produce nickel titanate "powder," not for the "film." In 2001, Chao and colleagues produced $NiTiO_3$ thin films by physical vapor deposition of Ti and Ni films, followed by direct thermal oxidation at 700°C under a diluted oxygen atmosphere.[24] Phani and Santucci prepared a single-phase crystalline structure of $NiTiO_3$ at 1000°C in 2001 using the sol–gel spin coating technique.[25] In 2005, Ohya *et al.*[26] used the dip-coating method and discovered $NiTiO_3$ forms in the interface between subsequently deposited layers of TiO_2 and NiO on ITO, leaving an $NiO/NiTiO_3/TiO_2/ITO$ structure, in that order. The current research fabricated thin films of a high-*k* dielectric material, nickel titanate, on silicon substrates by a modified sol–gel spin-coating method involving a sol-like solution as the precursor, followed by post-heat treatment at low temperatures. This study also investigated dielectric characteristics.

II. Experimental Procedure

(1) Preparation of the Precursor Solutions

Titanium isopropoxide [$Ti(O^iPr)_4$] (98+%, Acros Organics, Morris Plains, NJ), nickel acetate tetrahydrate [$Ni(OOCCH_3)_2 \cdot 4H_2O$] (99.0%, Showa Chemical Co., Tokyo, Japan), ethanol (99.5%, Echo Chemical Co., Miaoli, Taiwan), 2-porpanol (99.8%, Tedia Co., Fairfield, OH), ethylene glycol (99+%, Acros Organics), 1,2-dimethoxyethane (99+%, Acros Organics), and 2-methoxyethanol (99+%, Acros Organics) were used without further purification. $Ti(O^iPr)_4$ (16.7 mmol, 4.75 g) and $Ni(OOCCH_3)_2 \cdot 4H_2O$ (16.7 mmol, 4.16 g) were dissolved separately in 15 mL of different solvents (ethanol, 2-porpanol, ethylene glycol, 1,2-dimethoxyethane, and 2-methoxyethanol) and then mixed. The solution mixture was stirred at room temperature overnight, while the solution gradually turned to a transparent green color (2-methoxyethanol) or cloudy green color (ethanol, 2-porpanol, ethylene glycol, and 1,2-dimethoxyethane). The final concentration of the precursor solutions was 0.1*M* and the ratio of $Ti(O^iPr)_4$ and $Ni(OOCCH_3)_2 \cdot 4H_2O$ was 1:1.

(2) Preparation of Powders

Two milliliter of each precursor was placed in alumina boats for a two-stage heat-treatment process. First, the solution was heated to around 10°C lower than the b.p. temperature of the solvent. After most solvent was removed, the sample was post-heat treated at 600°C for 2 h. The final powder products were light yellow or yellow color.

(3) Preparation of Thin Films

Thin films of the 2-methoxyethanol precursor were spin-coated on SiO_2/Si substrates. The substrates were washed with

D. Damjanovic—contributing editor

Manuscript No. 27557. Received February 11, 2010; approved July 7, 2010.
This work was financially supported by the National Science Council of the Republic of China under grant no. NSC 96-2113-M-390-003.
[†]Author to whom correspondence should be addressed. e-mail: shchuang@nuk.edu.tw

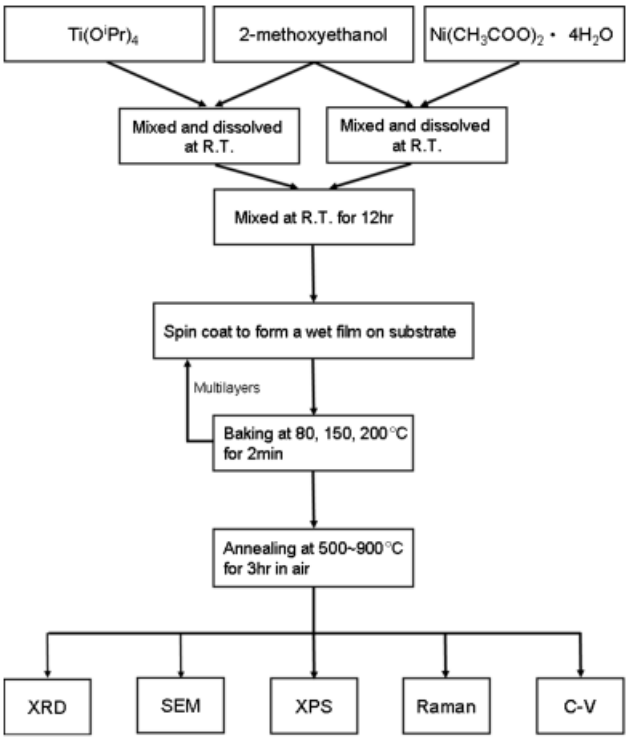

Fig. 1. The schematic flow chart of the nickel titanate thin film synthesis by a modified sol–gel method.

isopropyl alcohol, acetone, rinsed with distilled water, and transferred into the spin coating chamber for deposition. After spin coating of the precursor on the substrates, the films were baked at 80°, 150°, and 200°C for 2 min in air to remove the solvent. The procedure was repeated 10 times. In the post-heat treatment step, the thin films were annealed at different temperatures ranging from 500° to 900°C for 3 h in air. Figure 1 shows the details of the nickel titanate thin-film preparation method.

(4) Thin-Film Characterization

Field-emission scanning electron microscope (FE-SEM) analysis of film thickness and morphology was performed using the JEOL-6330 (JEOL Ltd., Tokyo, Japan). X-ray diffraction (XRD) was performed using the Bruker D8 ADVANCE (Bruker Co., Billerica, MA) and Rigaku Multiflex (Rigaku Co., Tokyo, Japan) using Cu$K\alpha$ radiation to identify film and powder structures. Analysis of elemental compositions and chemical bonding characteristics of the thin films was conducted with X-ray photoelectron spectroscopy (XPS, PHI 1600, Mg$K\alpha$, Physical Electronics Inc., Chanhassen, MN). Charge correction for carbon contamination was applied to the binding energies, with the binding energy of C 1*s* measured to be 284.5 eV. Raman spectroscopy was carried out with the Renishaw inVia Raman (Renishaw plc, Gloucestershire, U.K.) using a 514 nm laser radiation. The high-frequency capacitance–voltage (*C–V*) measurement was performed using an HP 4284A LCR meter (Agilent Technologies Inc., Santa Clara, CA). The dielectric constant was extracted from $C = \varepsilon_0\, \varepsilon_r\, A/d$, where ε_0 is the permittivity in vacuum $= 8.85 \times 10^{-14}$ F/cm, ε_r is the dielectric constant of $NiTiO_3$, A is the area of the electrode, and d is the thickness of the dielectric ($NiTiO_3$).

III. Results and Discussion

(1) Solvent Studies

We investigated a simple way of preparing $NiTiO_3$ at 600°C using different precursors. Five precursors with different solvents (ethanol, 2-porpanol, ethylene glycol, 1,2-dimethoxyethane, and 2-methoxyethanol) were prepared and examined. To analyze the crystal phases, XRD studies were performed. Figure 2 shows the XRD patterns of the powder samples obtained from precursors

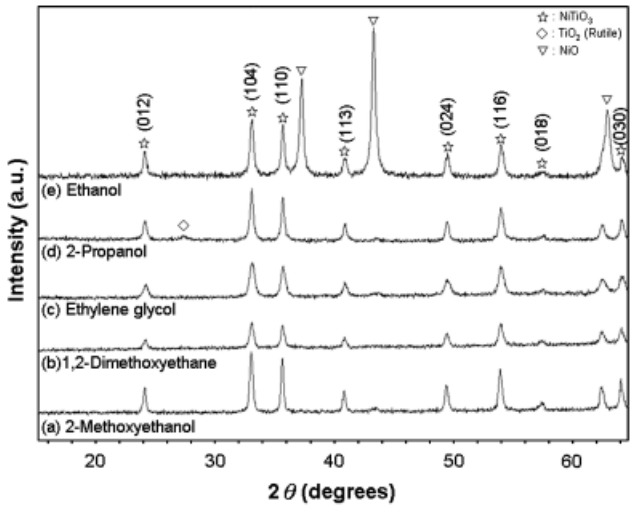

Fig. 2. X-ray diffraction patterns of the powders with different solvents post-heat treated at 600°C (a) 2-methoxyethanol, (b) 1,2-dimethoxyethane, (c) ethylene glycol, (d) 2-porpanol, and (e) ethanol.

with different solvents that were heat-treated at 600°C. Figures 2(a)–(c) show that, using 2-methoxyethanol, 1,2-dimethoxyethane, and ethylene glycol as the solvents, respectively, precursors produced powders with a single-phase $NiTiO_3$. Figure 2(d) shows that, with 2-porpanol as the solvent, the precursor produced a powder consisting mainly of $NiTiO_3$ with a trace of rutile TiO_2. Using ethanol as the solvent, the powder yielded after the heat treatment shows strong peaks corresponding to the major presence of NiO and smaller peaks corresponding to the minor presence of $NiTiO_3$ (Fig. 2(e)). Using ethanol or 2-propanol as the solvent seems to partially inhibit the formation of $NiTiO_3$. The correct choice of solvent, namely 2-methoxyethanol, 1,2-dimethoxyethane, and ethylene glycol, can correct this problem and yield single-phase $NiTiO_3$. These solvents may be acting as chelating agents,[27] thus suppressing other reaction pathways such as the formation of TiO_2 from Ti(O^{i}Pr)$_4$ and NiO from $Ni(OOCCH_3)_2 \cdot 4H_2O$. As a result, the rate for the reaction pathway leading to the formation of the binary metal oxide, $NiTiO_3$, is higher than that of the two former reaction pathways. However, when 1,2-dimethoxyethane or ethylene glycol was used as the solvent, the resulting precursor was a gel precursor that can be used to produce "powders" but not films. The precursor produced using 2-methoxyethanol as the solvent was a sol precursor that can be used to produce "films" in addition to powders. We therefore chose to use the 2-methoxyethanol precursor to produce thin films for this study.

(2) XRD and SEM Studies

Figure 3 shows the XRD patterns obtained at various temperatures of post-heat treatment of the films. The XRD peaks of films annealed at 500° and 550°C were broad as shown in Figs. 3(a) and (b), which could be identified as amorphous phases. At an annealing temperature of 600°C, all diffraction peaks were well-defined and, with reference to JCPDS card 17-0617 (rhombohedral, a = b = 5.03 Å, c = 13.786 Å), showed reflections of (012), (104), (110), (113), (024), (116), (018), (214), and (030) at 24.09°, 33.02°, 35.61°, 40.82°, 49.43°, 53.97°, 57.47°, 62.41°, and 64.09°, respectively. Lattice parameters of rhombohedral structure are a = b = 5.03 Å, and c = 13.809 Å. These diffraction peaks indicate the presence of anisotropic single-phase ilmenite $NiTiO_3$ in the products, not isotropic as $NiTiO_3$ powder. With the increasing temperature of post-heat treatment, the film tends to grow more in the (104) plane. The size of the crystallite $NiTiO_3$ was calculated by the Scherrer's formula.[28]

$$D_{XRD} = \frac{k \cdot \lambda}{B \cdot \cos\theta}$$

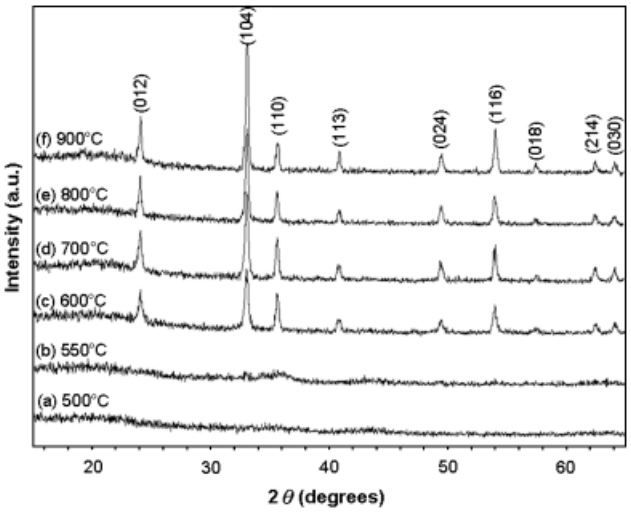

Fig. 3. X-ray diffraction patterns of the films with different post-heat treatment (a) 500°C, (b) 550°C, (c) 600°C, (d) 700°C, (e) 800°C, and (f) 900°C.

where B is the width at half maximum of the diffraction peaks, θ is the diffraction angle, D_{XRD} is the size of the crystallite, $k(0.9)$ is a constant, and λ(1.5418Å) is the wavelength of the X-ray Cu$K\alpha$ source. The crystallite sizes were calculated to be 30, 33, 36, and 40 nm at 600°, 700°, 800°, and 900°C, respectively. $NiTiO_3$ crystallite size increased with the increasing temperature. 600°C is the lowest reported temperature for the formation of single-phase $NiTiO_3$ thin film by the sol–gel method.

Figures 4(a) through (f) are the SEM images from the top of the films on SiO_2/Si substrates annealed between 500° and 900°C for 3 h in air. The images show that the surface of films was smooth and the particle size increased with the increasing annealing temperature. The mean particle sizes were calculated to be 38.6, 57.8, 79.4, and 110.5 nm at 600°, 700°, 800°, and 900°C, respectively. The crystallite sizes also show the same trend by XRD method. It is possible because mobility was great at high temperature and degree of freedom during nucleation was also great. Thickness of the films annealed at 500°, 550°, 600°, 700°, 800°, and 900°C determined by the SEM cross-sectional view were 194, 203, 185, 158, 145, and 121 nm, respectively. The film thickness increased from 194 to 203 nm as annealing temperature went from 500° to 550°C, possibly due to the oxygen in the air. When the annealing temperature was raised past 550°C, the cross-sectional view shows the films becoming thinner and denser with the increasing posttreatment temperature. This matches the sol–gel process results.

(3) XPS and Raman Studies

The major components of the film surfaces determined by XPS sample surveys were nickel, titanium, and oxygen. Figures 5 and 6 show high-resolution XPS at the Ni 2p and Ti 2p region of films at different posttreatment temperatures. Figure 5 also shows the shake-up structures of Ni, which suggest ligand-to-metal charge transfers.[29] Broad satellite peaks are found at approximately 861.3 ($2p_{3/2}$) and 878.5 eV ($2p_{1/2}$). For films posttreated between 500° and 900°C, the high-resolution XPS at the nickel region shows $2p_{3/2}$ and $2p_{1/2}$ signals at 855.2–855.4 eV and 872.7–873.1 eV, while the $2p_{3/2}$ and $2p_{1/2}$ signals were at 457.7–458.1 and 463.4–463.6 eV at the titanium region, respectively. During sputtering, some nickel atoms transformed to the metallic state, consistent with previously reported findings on $CoTiO_3$ and TaO_2.[30]

For film posttreated at 900°C, the binding energies of Ni and Ti were 855.2 ($2p_{3/2}$) and 457.7 eV ($2p_{3/2}$), respectively. The binding energy of Ni $2p_{3/2}$ in pure NiO was 856 eV and Ti $2p_{3/2}$ in rutile TiO_2 was 458.2 eV.[31] The decrease in Ni 2p and Ti 2p binding energies may be attributed to the weakening of Ni–O and Ti–O bonds due to formation of Ni–O–Ti bonds. For Ni $2p_{3/2}$ and Ti $2p_{3/2}$ in $NiTiO_3$ films, the binding energies shifted lower with an increased post-heat treatment temperature. This may be due to the increased crystallinity resulting from higher annealing temperatures, which can lead to the decreased distance between layers. Subsequently, the interaction forces between layers can increase, leading to the weakening of Ni–O–Ti bonds within individual layers.[32] The XRD data are also consistent with the above results.

Figure 7 shows the Raman spectra in the 200–800 cm^{-1} range for the $NiTiO_3$ films with posttreatment temperatures between 500° and 900°C for 3 h in air. In the case of ilmenite-type compounds, 10 Raman active modes ($5A_g+5E_g$) were observed and assigned to C_{3i}^2 symmetry and $R\bar{3}$space group.[23,33] Figures 7(a) and (b) show Raman spectra of the films with post-heat treatment at 500° and 550°C. No Raman active modes of $NiTiO_3$ are apparent, indicating either a high level of structural disorder in

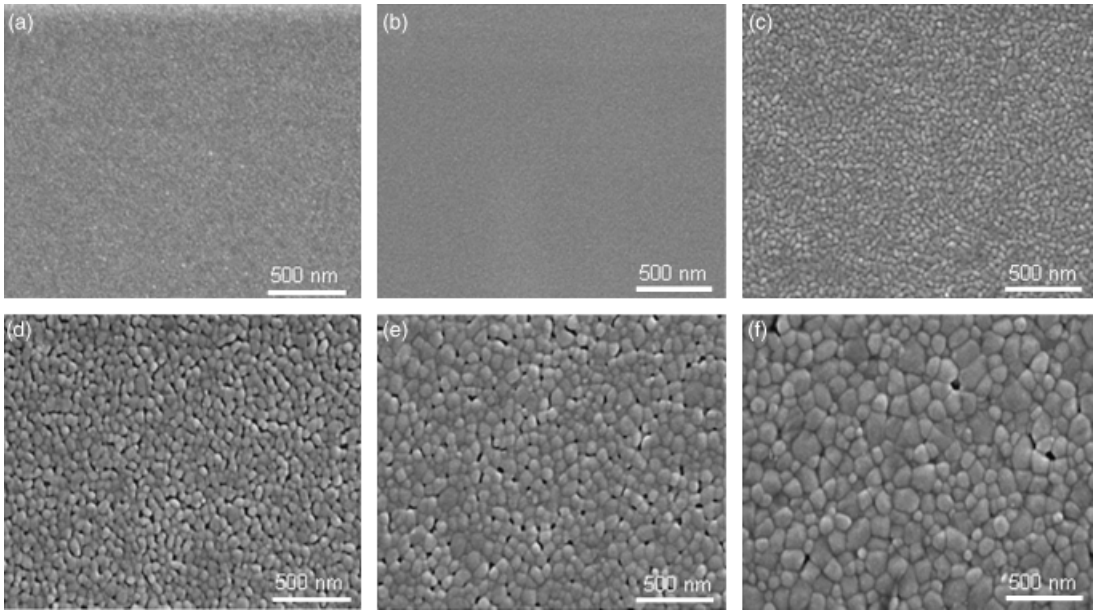

Fig. 4. Scanning electron microscopic images of the films with different post-heat treatment (a) 500°C, (b) 550°C, (c) 600°C, (d) 700°C, (e) 800°C, and (f) 900°C.

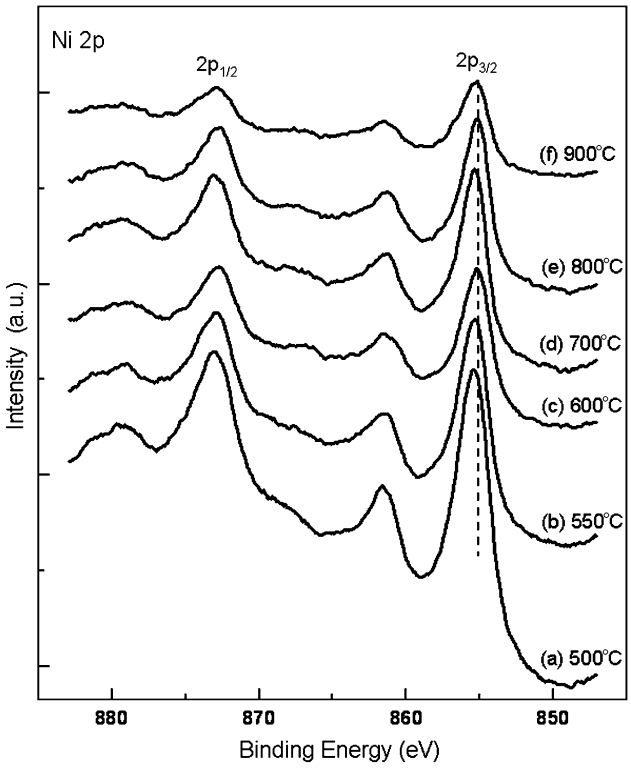

Fig. 5. Ni 2*p* XPS spectra of the films with different post-heat treatment (a) 500°C, (b) 550°C, (c) 600°C, (d) 700°C, (e) 800°C, and (f) 900°C.

the short range or no $NiTiO_3$ structure in the films. In Fig. 7(c), it appears that post-heat treatment temperatures at 600°C showed a low intensity of Raman active peaks, confirming the short range of structural order in the film. Figures 7(c)–(f) show that stronger Raman peaks were observed with the increasing post-heat treatment temperature, indicating higher structural order. Films with post-heat treatment temperatures higher than

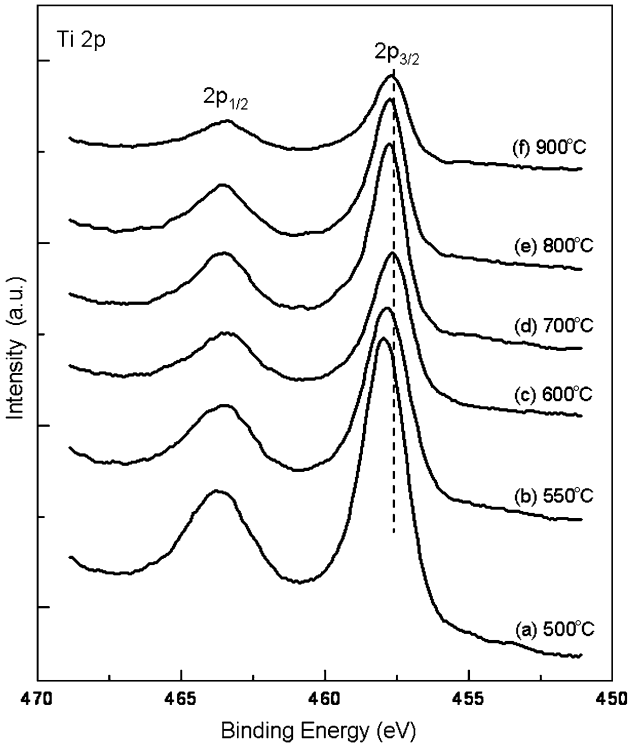

Fig. 6. Ti 2*p* XPS spectra of the films with different post-heat treatment (a) 500°C, (b) 550°C, (c) 600°C, (d) 700°C, (e) 800°C, and (f) 900°C.

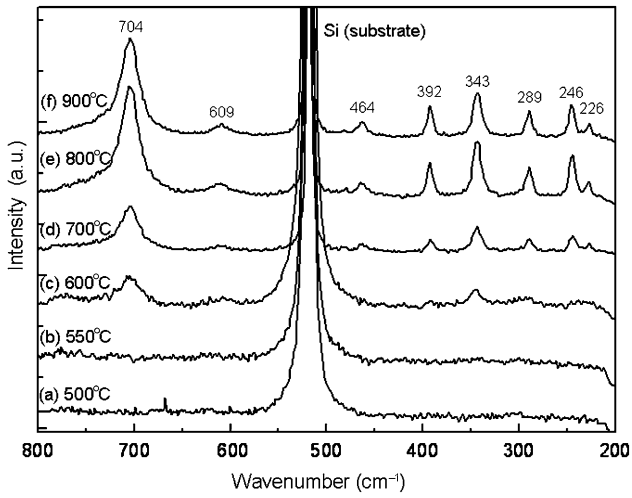

Fig. 7. Raman spectra of the films with different post-heat treatment (a) 500°C, (b) 550°C, (c) 600°C, (d) 700°C, (e) 800°C, and (f) 900°C.

550°C obtained eight of 10 Raman active modes. The peaks are at 226, 246, 289, 343, 392, 464, 609, and 704 cm^{-1}. The lost peaks can be attributed to low intensity or their lack of presence in this area. These Raman results agree with the XRD results and the literature.[23]

(4) Dielectric Permittivity Studies

To estimate the dielectric constant of $NiTiO_3$ thin film, this study used thermal oxidation to grow a high-quality SiO_2 thin film first. Then, the $NiTiO_3$ dielectric film was spun on the wafer and annealed at 600°C under nitrogen for 30 s by RTA method. Figure 8 shows the *C–V* characteristics of both the $Si/SiO_2/NiTiO_3/TaN$, and $Si/SiO_2/TaN$ capacitors. Well-behaved *C–V* characteristics were observable for both capacitors without flat-band voltage shift. The capacitance equivalent thickness (CET) was extracted from *C* to *V* curves at 100 kHz without considering quantum and depletion effects from the silicon substrate. The CET of gate dielectric layers of $SiO_2/NiTiO_3$ and SiO_2 structures were 6.59 and 5.27 nm, respectively. The physical thicknesses of 1-coated high-*k* dielectric $NiTiO_3$ and thermal oxide were 14.0 and 5 nm, respectively. As a result, the exact dielectric constant of the $NiTiO_3$ thin film was calculated to be 41.36, which was higher than $NiTiO_3$ powder in the literature ($\sim$15.5).[34] This is possibly due to the relatively lower number of defects present in the film. The dielectric constant of the $NiTiO_3$ film is close to the films that were fabricated by directly thermal

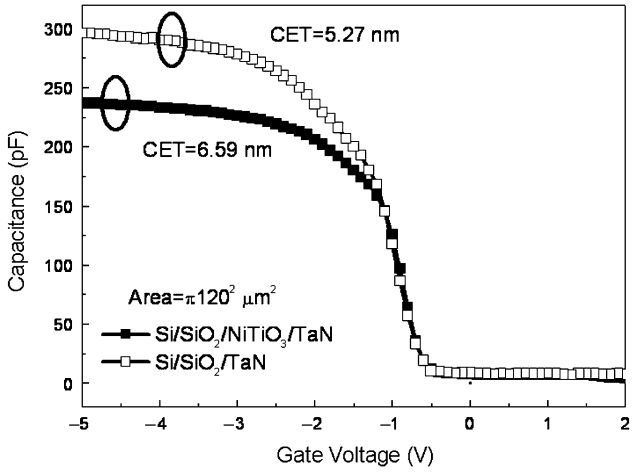

Fig. 8. *C–V* curves of capacitors with $Si/SiO_2/NiTiO_3/TaN$ and $Si/SiO_2/TaN$ stack structures.

oxidizing the deposited Ni/Ti films formed by the physical vapor deposition method.[24]

IV. Conclusions

This study successfully produced high-quality nickel titanate thin films at low temperatures. $NiTiO_3$ thin films were deposited on SiO_2/Si(100) by the spin coating sol–gel method using titanium isopropoxide, nickel acetate tetrahydrate, and 2-methoxyethanol. The single-phase $NiTiO_3$ was observable by XRD when the films were annealed at and above 600°C. The film morphologies were smooth as confirmed by SEM. The XPS and Raman analysis also indicated the films were of $NiTiO_3$ when annealed at and above 600°C. In summary, we were able to produce the single-phase $NiTiO_3$ films at the lowest processing temperature currently known. Future applications of this high-*k* film in the semiconductor industry are promising.

References

[1]Z. Tang, Z. Zhou, and Z. Zhang, "Experimental Study on the Mechanism of $BaTiO_3$-Based PTC–CO Gas Sensor," *Sens. Actuat. B*, **93**, 391–5 (2003).

[2]M. Siemons and U. Simon, "Gas Sensing Properties of Volume-Doped $CoTiO_3$ Synthesized via Polyol Method," *Sens. Actuat. B*, **126**, 595–603 (2007).

[3]Q. Zhu, W. Y. Shih, and W. H. Shih, "Real-Time, Label-Free, All-Electrical Detection of Salmonella Typhimurium Using Lead Titanate Zirconate/Gold-coated Glass Cantilevers at Any Relative Humidity," *Sens. Actuat. B*, **125**, 379–88 (2007).

[4]S. H. Xiao, H. J. Xu, J. Hu, W. F. Jiang, and X. J. Li, "Structure and Humidity Sensing Properties of Barium Strontium Titanate/Silicon Nanoporous Pillar Array Composite Films," *Thin Solid Films*, **517**, 929–32 (2008).

[5]R. A. Potyrailo and V. M. Mirsky, "Combinatorial and High-Throughput Development of Sensing Materials: The First 10 Years," *Chem. Rev.*, **108** [2] 770–813 (2008).

[6]G. Radnóczi, P. B. Barna, M. Adamik, Z. Czigány, J. Ariake, N. Honda, and K. Ouchi, "Growth Structure of Thin Films for Perpendicular Magnetic Recording Media," *Cryst. Res. Technol.*, **35** [6–7] 707–11 (2000).

[7]K. Tohji, Y. Udagawa, S. Tanabe, T. Ida, and A. Ueno, "Catalyst Preparation Procedure Probed by EXAFS Spectroscopy. 2. Cobalt on Titania," *J. Am. Chem. Soc.*, **106** [18] 5172–8 (1984).

[8]L. Chen, S. Zhang, L. Wang, D. Xue, and S. Yin, "Preparation and Photocatalytic Properties of Strontium Titanate Powders via Sol–Gel Process," *J. Cryst. Growth*, **311**, 746–8 (2009).

[9]Y. Ni, X. Wang, and J. Hong, "Nickel Titanate Microtubes Constructed by Nearly Spherical Nanoparticles: Preparation, Characterization and Properties," *Mater. Res. Bull.*, **44**, 1797–801 (2009).

[10]M. Zheng, X. Xing, J. Deng, L. Li, J. Zhao, L. Qiao, and C. Fang, "Synthesis and Characterization of (Zn,Mn)TiO_3 by Modified Sol–Gel Route," *J. Alloys Compd.*, **456**, 353–7 (2008).

[11]B. Cheng, M. Cao, P. V. Voorde, W. Greene, H. Stork, Z. Yu, and J. C. S. Woo, "Design Considerations of High-*k* Gate Dielectrics for Sub-0.1-μm MOSFET's," *IEEE Trans. Electron Devices*, **46** [1] 261–2 (1999).

[12]T. M. Pan, T. F. Lei, and T. S. Chao, "High-*k* Cobalt–Titanium Oxide Dielectrics Formed by Oxidation of Sputtered Co/Ti or Ti/Co Films," *Appl. Phys. Lett.*, **78** [10] 1439–41 (2001).

[13]J. H. Chen, T. B. Huang, X. Wu, D. Landheer, T. F. Lei, and T. S. Chao, "Performance Improvement of $CoTiO_3$ High-*k* Dielectrics with Nitrogen Incorporation," *J. Electrochem. Soc.*, **154** [1] G18–23 (2007).

[14]Y. Gao, Y. Masuda, T. Yonezawa, and K. Koumoto, "Site-Selective Deposition and Micropatterning of $SrTiO_3$ Thin Film on Self-Assembled Monolayers by the Liquid Phase Deposition Method," *Chem. Mater.*, **14** [12] 5006–14 (2002).

[15]Y. Gan, Q. J. Cai, C. M. Li, H. B. Yang, Z. S. Lu, C. Gong, and M. B. Chan-Park, "Solution-Prepared Hybrid-Nanoparticle Dielectrics for High-Performance Low-Voltage Organic Thin-Film Transistors," *ACS Appl. Mater. Interfaces*, **1** [10] 2230–6 (2009).

[16]X. Du, Y. Xu, H. Ma, J. Wang, and X. Li, "Low-Temperature Synthesis of Bismuth Titanate by an Aqueous Sol–Gel Method," *J. Am. Ceram. Soc.*, **91** [7] 2079–82 (2008).

[17]P. R. Evans, X. H. Zhu, P. Baxter, M. McMillen, J. McPhillips, F. D. Morrison, J. F. Scott, R. J. Pollard, R. M. Bowman, and J. M. Gregg, "Toward Self-Assembled Ferroelectric Random Access Memories: Hard-Wired Switching Capacitor Arrays with Almost Tb/in.^{2} Densities," *Nano Lett.*, **7** [5] 1134–7 (2007).

[18]D.-Y. Wang, C.-H. Chien, C.-Y. Chang, C.-C. Leu, J.-Y. Yang, S.-H. Chuang, and T.-Y. Huang, "Low-Pressure Crystallization of Sol–Gel-Derived $PbZr_{0.52}Ti_{0.48}O_3$ Thin Films at Low Temperature for Low-Voltage Operation," *Jpn. J. Appl. Phys.*, **42** [5A] 2756–8 (2003).

[19]E. M. Alkoy, C. Dagdeviren, and M. Papila, "Processing Conditions and Aging Effect on the Morphology of PZT Electrospun Nanofibers, and Dielectric Properties of the Resulting 3–3 PZT/Polymer Composite," *J. Am. Ceram. Soc.*, **92** [11] 2566–70 (2009).

[20]Y.-J. Lin, Y.-H. Chang, W.-D. Yang, and B.-S. Tsai, "Synthesis and Characterization of Ilmenite $NiTiO_3$ and $CoTiO_3$ Prepared by a Modified Pechini Method," *J. Non-Cryst. Solids*, **352**, 789–94 (2006).

[21]A. E. Henkes, J. C. Bauer, A. K. Sra, R. D. Johnson, R. E. Cable, and R. E. Schaak, "Low-Temperature Nanoparticle-Directed Solid-State Synthesis of Ternary and Quaternary Transition Metal Oxides," *Chem. Mater.*, **18** [2] 567–71 (2006).

[22]M. S. Sadjadi, K. Zare, S. Khanahmadzadeh, and M. Enhessari, "Structural Characterization of $NiTiO_3$ Nanopowders Prepared by Stearic Acid Gel Method," *Mater. Lett.*, **62**, 3679–81 (2008).

[23]K. P. Lopes, L. S. Cavalcante, A. Z. Simões, J. A. Varela, E. Longo, and E. R. Leite, "$NiTiO_3$ Powders Obtained by Polymeric Precursor Method: Synthesis and Characterization," *J. Alloys Compd.*, **468**, 327–32 (2009).

[24]T. M. Pan, T. F. Lei, and T. S. Chao, "Comparison of Ultrathin $CoTiO_3$ and $NiTiO_3$ High-k Gate Dielectrics," *J. Appl. Phys.*, **89** [6] 3447–52 (2001).

[25]A. R. Phani and S. Santucci, "Structural Characterization of Nickel Titanium Oxide Synthesized by Sol–Gel Spin Coating Technique," *Thin Solid Films*, **396**, 1–4 (2001).

[26]Y. Ohya, T. Niwa, T. Ban, and Y. Takahashi, "Rectifying Properties of Oxide Semiconductor Heterostack Films at Elevated Temperatures," *J. Sol–Gel Sci. Technol.*, **33**, 323–6 (2005).

[27]B. L. Cushing, V. L. Kolesnichenko, and C. J. O'Connor, "Recent Advances in the Liquid-Phase Syntheses of Inorganic Nanoparticles," *Chem. Rev.*, **104** [9] 3893–946 (2004).

[28]B. D. Cullity and S. R. Stock, *Elements of X-Ray Diffraction.* Prentice-Hall Inc., New Jersey, 2001 170pp.

[29]J. F. Moulder, W. F. Stickle, P. E. Sobol, and K. D. Bomben, *Handbook of X-Ray Photoelectron Spectroscopy*, pp. 18–20. Perkin-Elmer Corp., Minnesota, 1992.

[30]H.-T. Chiu, C.-N. Wang, and S.-H. Chuang, "Metal-Organic CVD of Tantalum Oxide from Tert-Butylimidotris(diethylamido)tantalum and Oxygen," *Chem. Vap. Deposition.*, **6** [5] 223–5 (2000).

[31]S. Zhang, J. Wang, and X. Wang, "Effect of Calcination Temperature on Structure and Performance of Ni/TiO_2–SiO_2 Catalyst for CO_2 Reforming of Methane," *J. Nat. Gas Chem.*, **17** [2] 179–83 (2008).

[32]G.-W. Zhou, D. K. Lee, Y. H. Kim, C. W. Kim, and Y. S. Kang, "Preparation and Spectroscopic Characterization of Ilmenite-Type $CoTiO_3$ Nanoparticles," *Bull. Korean Chem. Soc.*, **27** [3] 368–72 (2006).

[33]M. I. Baraton, G. Busca, M. C. Prieto, G. Ricchiardi, and V. S. Escribano, "On the Vibrational Spectra and Structure of $FeCrO_3$ and of the Ilmenite-Type Compounds $CoTiO_3$ and $NiTiO_3$," *J. Solid State Chem.*, **112**, 9–14 (1994).

[34]J. Luo, X. Xing, R. Yu, Q. Xing, G. Liu, D. Zhang, and X. Chen, "Low-Temperature Synthesis and Characterization of (Zn,Ni)TiO_3 Ceramics by a Modified Sol–Gel Route," *J. Alloys Compd.*, **420**, 317–21 (2006). □